iScience

CellPress

Article

Wnt Signaling Directs Neuronal Polarity and Axonal Growth

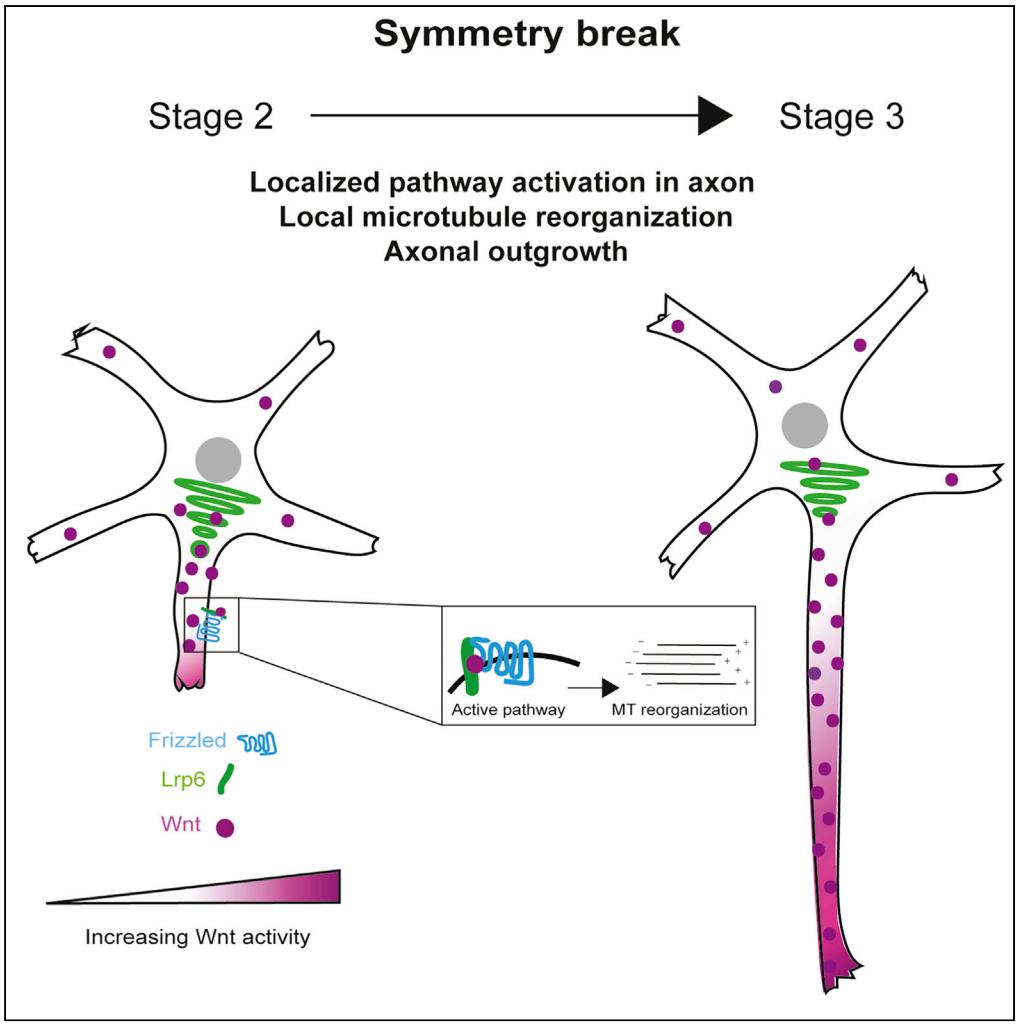

Eliana Stanganello, Eitan Erez Zahavi, Mithila Burute, ..., Madelon M. Maurice, Lukas C. Kapitein, Casper C. Hoogenraad

c.hoogenraad@uu.nl

HIGHLIGHTS

Wnt3a distributes asymmetrically in early stages neurons

A spatially localized Wnt3a source determines axon positioning and early guidance

Concentration gradient of Wnt3a guides axonal outgrowth across a microfluidic chamber

Wnt3a directly controls microtubules remodeling

Stanganello et al., iScience *13*, 318–327
March 29, 2019
https://doi.org/10.1016/j.isci.2019.02.029

iScience

CellPress

Article

Wnt Signaling Directs Neuronal Polarity and Axonal Growth

Eliana Stanganello,[1] Eitan Erez Zahavi,[1] Mithila Burute,[1] Jasper Smits,[1] Ingrid Jordens,[2] Madelon M. Maurice,[2] Lukas C. Kapitein,[1] and Casper C. Hoogenraad[1,3,*]

SUMMARY

The establishment of neuronal polarity is driven by cytoskeletal remodeling that stabilizes and promotes the growth of a single axon from one of the multiple neurites. The importance of the local microtubule stabilization in this process has been revealed however, the external signals initiating the cytoskeletal rearrangements are not completely understood. In this study, we show that local activation of the canonical Wnt pathway regulates neuronal polarity and axonal outgrowth. We found that in the early stages of neuronal polarization, Wnt3a accumulates in one of the neurites of unpolarized cells and thereby could determine axon positioning. Subsequently, Wnt3a localizes to the growing axon, where it activates the canonical Wnt pathway and controls axon positioning and axonal length. We propose a model in which Wnt3a regulates the formation and growth of the axon by activating local intracellular signaling events leading to microtubule remodeling.

INTRODUCTION

The transition from stage 2 to stage 3 is a fundamental step during neuronal development, which determines neuron polarization in culture (Dotti et al., 1988). At stage 2, neurons are characterized by multiple neurites with a similar length. A growth advantage of one of the neurites over the others defines the transition to the stage 3 in which the axon starts to form. It has been shown that cytoskeletal remodeling such as local microtubule stabilization play a fundamental role in this process (Kapitein and Hoogenraad, 2015). However, the external signals responsible for this growth advantage are not yet completely understood. The Wnt family of proteins are known regulators of a broad spectrum of developmental processes (van Amerongen and Nusse, 2009). Wnt proteins form instructive gradients within the central nervous system and have a fundamental role in maintaining progenitor cells and granting neurogenesis (Machon et al., 2007). Furthermore, Wnt is a known regulator of cell polarity and has also been shown to be a symmetry-breaking factor in proliferating cells (Habib et al., 2013). Clustering of canonical Wnt ligands at the plasma membrane can trigger the outgrowth of cell protrusions during neural plate patterning in zebrafish (Stanganello et al., 2015).

Wnt3a is the best characterized canonical Wnt ligand with a fundamental role in the specification of the hippocampus (Lee et al., 2000); therefore, we focused our attention in this study on Wnt3a as a representative for canonical Wnt proteins. We hypothesize that canonical Wnt signaling is involved in the early stages of symmetry breaking and axon outgrowth in hippocampal neurons.

RESULTS AND DISCUSSION

Wnt Signaling Is Active in the Axon

We first examined localization of endogenous Wnt3a at different neuronal stages. As shown in Figure 1A, Wnt3a accumulates in one of the neurites of stage 2 neurons (48% of neurons analyzed; n = 27) and later on localizes to the longest neurite, i.e., the future axon of stage 3 (76% of the neurons; n = 21) and stage 4 (60% of the neurons; n = 20) neurons. To verify the specificity of the Wnt3a antibody staining we performed immunofluorescence in neurons overexpressing Wnt3a, Wnt5a, and Wnt8b and found that it specifically detects Wnt3a (Figure S1A). To verify that Wnt indeed localizes at the axon, we performed a co-staining with Tau, a microtubule-binding protein that serves as axonal marker (Figure S1B). A model proposed for symmetry breaking is the "local activation model," in which a local signal is necessary and sufficient to induce axonal outgrowth (Inagaki et al., 2011). The asymmetric distribution of Wnt3a in early stages of neuronal development (Figure 1A) fits the local activation model, suggesting a role of canonical Wnts in polarity establishment. Thus, we analyzed whether the accumulation of Wnt proteins also leads to a local activation of the canonical Wnt pathway. One of the first molecular events occurring during the activation of

[1]Cell Biology, Department of Biology, Faculty of Science, Utrecht University, Padualaan 8, 3584 CH Utrecht, The Netherlands

[2]Oncode Institute, Cell Biology, Center for Molecular Medicine, University Medical Center Utrecht, Utrecht, The Netherlands

[3]Lead Contact

*Correspondence: c.hoogenraad@uu.nl

https://doi.org/10.1016/j.isci.2019.02.029

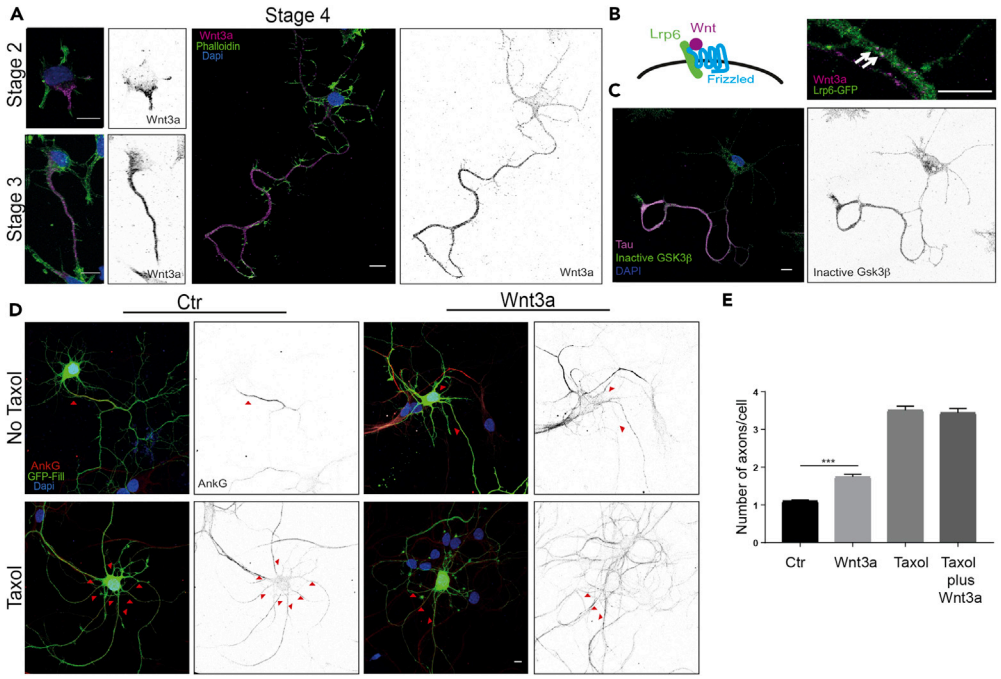

Figure 1. Enrichment of Wnt3a at the Growing Axon and a Local Activation of the Pathway Regulate Axonal Formation

(A) Endogenous Wnt3a expression at stages 2, 3, and 4 of neuronal development. Neurons were fixed at the indicated time points and stained with an antibody against Wnt3a (magenta). Neurons were counterstained with Phalloidin (actin filaments; green) and DAPI (nuclei; blue) (left side: merged picture; right side: inverted gray-scale channel of the endogenous Wnt3a expression [scale bar, 10 μm]).

(B) Left side: Schematic representation of a Wnt signalosome. Wnt binding induces clustering of Wnt ligands and its receptors Frizzled and LRP6. Right side: Neurons were transfected with Lrp6-GFP at Div3, fixed at Div4, and stained for the endogenous Wnt3a. Arrows indicate clustering and co-localization of Lrp6 (green) with Wnt3a (magenta) at the axon (scale bar, 10 μm).

(C) Gsk3β inactivation in the axon of stage 4 neurons. Neurons were fixed at stage 4 and subjected to an antibody staining against an inactivated form of Gsk3β (phospho-Gsk3β magenta). Neurons were counterstained with Phalloidin (actin filaments; green) and DAPI (nuclei; blue) (left side: merged picture; right side: inverted gray-scale channel of the phospho-Gsk3β signal) (scale bar, 10 μm).

(D) Neurons were co-transfected with GFP (to identify transfected neurons) and either an empty vector as a control (left panels) or an expression vector containing Wnt3 (right panels) at Div0. Neurons were either left untreated (upper panel) or treated with Taxol (10 nM, lower panel) at Div1. Neurons were fixed at Div 4 and stained for AnkG. Pictures on the left side show an overlay of GFP (green), AnkG (axonal initial segment; red), and DAPI (nuclei; blue). Pictures on the right show the inverted gray scale of the AnkG staining (scale bar, 10 μm). Red arrowheads indicate axons.

(E) Bar graph representing the average number of axons per neuron, determined by the number of axonal initial segments per cell (n = 20 ***$p < 0.0001$, mean (S.E.M) values are shown).

canonical Wnt signaling is the clustering of the co-receptor Lrp6 at the site of Wnt activation, leading to the formation of Wnt signalosomes (Bilic et al., 2007). We analyzed whether Wnt signalosomes form at the growing axon. Owing to the toxicity of Lrp6 when transfected at earlier stages, we transfected neurons at day *in vitro* (Div) 3 with an Lrp6-GFP construct and stained for the endogenous Wnt3a. The Wnt (co-) receptors Lrp6 and the receptor Frizzled-5 (Fz5) were evenly distributed in the cell. Co-localizations between Wnt3a and Lrp6-GFP, considered to be *bona fide* Wnt signalosomes, were found in the proximal axon (Figure 1B). Some Wnt signalosomes could also be observed in dendrites (Figures S1C and S1D). To know whether signalosome formation was Wnt dependent we examined the local dynamics of signalosomes at the axons. We imaged Lrp6-GFP at Div4 in control neurons and neurons that were treated with Wnt3a conditioned medium for 30 min. We detected enhanced signalosome formation, as demonstrated by Lrp6 punctae of increased size, whereas the total number of punctae did not change (Figures S2A–S2C). In addition, live imaging showed a higher turnover of Lrp6 punctae in Wnt-treated neurons compared with control neurons (Figures S2D and S2E, new punctae red arrowhead, disappearing punctae blue

arrowhead). These results indicate that Wnt3a enhances the formation of Wnt signalosomes to promote Wnt activity in the axon. Wnt signaling leads to the inhibition of Gsk3β by phosphorylation (Fukumoto et al., 2001). As Wnt signalosomes could be observed in the axon as well as in dendrites, we wanted to clarify whether activation of canonical Wnt signaling is specific to the axon. Indeed, we detected the inactive, phosphorylated form of Gsk3β in stage 4 neurons by immunofluorescence and found that Gsk3β is specifically inhibited in the axon, where Wnt3a is also localized (Figure 1C). When the Wnt signaling pathway is inhibited, by means of inhibiting its endogenous secretion in the culture by Iwp-2 or by inhibiting its activation of Lrp6 with Dkk1 (Bafico et al., 2001) this local Gsk3β inhibition is lost (Figure S2F). These results indicate that Wnt3a accumulation in the growing axon activates intracellular downstream signaling of the canonical Wnt pathway.

As endogenous Wnt3 accumulates and activates downstream signaling at the axon, we examined whether mislocalizing Wnt by its overexpression affected neuronal polarization by altering the formation of a single axon per neuron, a hallmark of hippocampal neuron polarity establishment (Dotti et al., 1988).

To this aim, we transfected neurons at Div0 either with a Wnt3 construct or the corresponding empty vector as a control. In both cases a GFP-expression construct was co-transfected to identify transfected cells. We fixed the neurons at Div4 and performed immunostaining for Ankyrin G (AnkG), a protein that is specifically localized in the axonal initial segment (AIS), to count the number of axons per neuron. As a positive control, neurons were treated with Taxol, a microtubule-stabilizing drug that induces multiple axons formation (Witte et al., 2008). The majority of neurons in the untreated control group developed only one axon per neuron. By contrast, neurons transfected with Wnt3 showed formation of multiple axons (on average 1.74 per neuron, n = 20) (Figures 1D and 1E). In neurons developing more than one axon under Wnt3a over-expression and Taxol treatments, AnkG was less concentrated in the AIS region of the axon and was more diffused along it (Figure 1D, depicted by red arrowheads). These results clearly indicate that Wnt overexpression interferes with neuronal polarization. Consistently, the intensity profile along the proximal axon of both AnkG and Trim46, another AIS protein, was lower in Wnt-overexpressing neurons compared with control neurons. These findings suggest a Wnt induced re-distribution of AIS proteins, most probably caused by the mislocalization of the Wnt signaling activity (Figures S2G–S2J). The effect of Wnt3 on neuronal polarity was not as strong as the effect of direct microtubules stabilization by Taxol, which resulted in an average of 3.51 (n = 20) axons per neuron (Figure 1E). A combination of Wnt3 overexpression and Taxol treatment did not further increase the axon multiplicity, suggesting that Wnt and Taxol promote axon formation via a similar mechanism.

Wnt Is Required for Establishment of Neuron Polarity

Wnt ligands are secreted, lipidated glycoproteins. In the Wnt-producing cell, Wnt is lipid-modified by Porcupine in the ER, an essential step for its further transport and secretion outside the cell (Bänziger et al., 2006; Bartscherer et al., 2006; Goodman et al., 2006; Kadowaki et al., 1996; Takada et al., 2006; Zhai et al., 2004) (Figure 2A). As we observed formation of multiple axons upon Wnt treatment, we further investigated the requirement of Wnt3a in neuronal polarity by inhibiting endogenous Wnt secretion with Iwp-2, a specific inhibitor of Porcupine. We treated neurons at Div0 with Iwp-2 and analyzed the localization of Wnt3a at Div4. In the control condition, endogenous Wnt3a localize to the cell body with enhanced levels in the axon (Figure 2B, left panels, overview; right panels, zoom-in cell body and axon). In Iwp-2-treated neurons, Wnt3a accumulates in the cell body and is depleted from the longest neurite (Figure 2B). Interestingly, we observed drastic mislocalization of Tau in Div2 neurons, without clear demarcation of the axon (Figures 2C and 2D). These neurites are also positive for the dendritic marker MAP2 (Figures S3A and S3B). This result suggests a crucial role for Wnt proteins in the establishment of axonal polarity. As Iwp-2 suppresses the secretion of all Wnt proteins, including non-canonical Wnts, we treated neurons with Iwp-2 in combination with recombinant Wnt3a, to address whether canonical Wnt signaling specifically can rescue the mislocalization of Tau by Iwp-2. In neurons treated with Wnt3a alone, accumulation of Tau in the cell body (blue arrows head) or multiple axons could be observed (red arrows heads) and indeed Wnt3a rescues axon formation in Iwp-2-treated neurons to the level of Wnt3a, confirming the effect of Wnt3a on neuronal polarity (Figures 2C and 2D). Neurons treated with Dkk1, a specific antagonist of Lrp6 that activates the canonical Wnt signaling, show a similar phenotype to those treated with Iwp-2, namely, a loss of Tau specificity and mislocalization to MAP2-positive neurites (Figures S3A and S3B). Together these results indicate an important role for localized activation of canonical Wnt signaling on neuronal polarity and axonal outgrowth at early stages of neuronal development. We therefore aimed

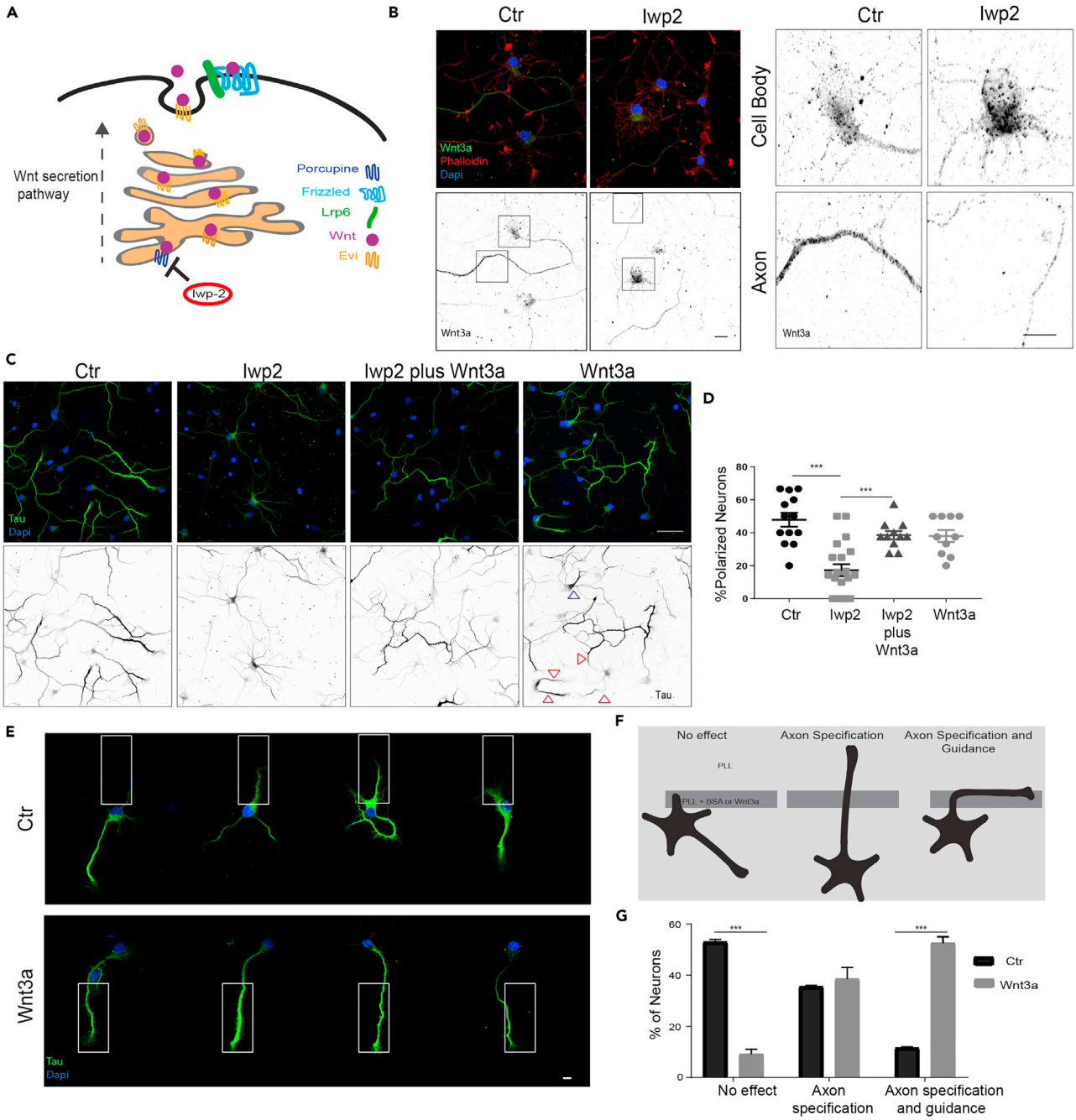

Figure 2. Localized Wnt3a Determines Axonal Formation and Positioning

(A) Schematic representation of the mode of action of Iwp-2. Iwp-2 blocks Porcupine-mediated lipid modification and consequently the secretion of Wnt proteins.

(B) Div0 neurons were either left untreated or treated with Iwp-2 (1 μM). Neurons were fixed at Div4 and stained for Wnt3a. Neurons were counterstained with Phalloidin (actin filaments; red) and DAPI (nuclei; blue) (upper panels: merged picture; lower panel: inverted gray-scale channel of the endogenous Wnt3a) (scale bar, 10 μm). Wnt3a accumulates peri-nuclear after treatment with Iwp-2 (upper panel), and the staining is decreased in the axon (lower panel) (scale bar, 10 μm).

(C) Neurons were either left untreated or treated at Div0 with Iwp-2 alone, Iwp-2 (1 μM) + Wnt3a (40 ng/mL), or Wnt3a alone. At Div2 neurons were fixed and stained for Tau and counterstained with DAPI. Upper panel: merged staining of Tau proteins (green) and nuclei (DAPI; blue). Lower panel: inverted gray scale of intensity of the antibody staining against Tau. Experimental conditions from left to right: untreated neurons, neurons treated with Iwp-2 alone, Iwp-2 in combination with recombinant WNT3a, and recombinant WNT3a alone. Pictures show representative results of at least three independent experiments (scale bar, 10 μm). Red arrowheads indicate multiple axons; blue arrowheads indicate Wnt retention of Tau in the cell body.

Figure 2. *Continued*

(D) Graph representing the percentage of cells with axonal localization of Tau in each quantified picture normalized to the number of nuclei present in the analyzed field (***p < 0.005, n = 20, mean (S.E.M) values are shown).

(E) Div0 neurons were seeded on a micro-patterned coverslip containing either a pattern of fluorescent BSA (control) or a pattern containing a mix of recombinant Wnt3a protein with BSA. The patterns are indicated by the white boxes. Neurons were fixed on the coverslip at Div2 and stained for Tau (green), and nuclei were counterstained with DAPI (blue). Upper panel: representative pictures of neurons on the control pattern. A montage of single neurons was made with ImageJ. Lower panel: representative pictures of neurons on the Wnt3a pattern. Pictures show representative results of at least three independent experiments (scale bar, 10 μm).

(F) Axon positioning of the neurons in (E) were divided into three categories: no effect, axon specification, and axon specification and guidance. Neurons are stained for Tau (green) and nuclei counterstained with DAPI (blue).

(G) Percentage of neurons belonging to different categories on BSA or Wnt3a + BSA patterned coverslips (n = 30, ***p < 0.0001, mean (S.E.M) values are shown).

to dissect the specific role that Wnt signaling plays in neuronal polarity and early axonal guidance, which is challenged by the complexity of the pathway, primarily the broad range of Wnt ligands and their receptors, as well as the cross talk between canonical and different non-canonical downstream pathways (Niehrs, 2012). To meet these challenges, we adopted simplified methods to further address specifically the role of canonical Wnt signaling as a local and directional cue regulating neuronal polarity and axonal growth.

Wnt Signaling Guides Axon Position and Growth

Extracellular signals are known to guide emergence of axons both *in vitro* and *in vivo* (Barnes and Polleaux, 2009). Wnt proteins can bind to extracellular matrix proteins and serve as extracellular signals (Yan and Lin, 2009). To investigate whether spatially localized Wnt proteins could guide axon emergence in developing neurons, we studied axonal outgrowth on micropatterns coated with Wnt3a. Neurons were seeded at Div0 on coverslips in which either BSA (control) or BSA together with recombinant Wnt3a were grafted in specific regions, whereas the remaining area of the coverslip was covered with poly-L-Lysine (Figure 2E). Forty-eight hours after seeding, the neurons were fixed and divided into three categories based on the position of the axon: (1) neurons contacted the BSA or Wnt3a micropatterns but did not form axons on these patterns; (2) axons contacted the micropatterns but continued to grow out of this region; (3) axons formed and grew along the area of the micropattern (Figure 2F). In both conditions, BSA alone or in combination with Wnt3a, approximately 35% of neurons showed axon specification on the micropattern but no axon guidance (category 2), which can occur when unspecified neurites detect a relative change in the substrate composition (Figure 2G). However, on the BSA-coated coverslips, less than 10% of the axons were guided by the micropattern (category 3). In contrast, in the Wnt3a-grafted micropatterns, 57% of the neurons (n = 30) positioned their axon and were guided by the pattern geometry compared with 16% (n = 47) in control (Figures 2E and 2G), suggesting that, in unpolarized neurons, extracellular Wnt3a determines axon formation and guides axonal outgrowth. Together these results show that a local source of Wnt3a can act as an external cue to control the axon specification and formation. Such an external asymmetric source of Wnt can be represented by Wnt bound to the extracellular matrix or delivered by other cells, e.g., glia cells or other neurons. These could locally contact the unpolarized neuron and deliver Wnt to one particular neurite thereby inducing pathway activation and consequently determining axonal outgrowth.

Wnt Function as Early Axonal Guidance Cue

Wnt proteins form instructive gradients within the central nervous system and have a fundamental role in maintaining progenitor cells and promoting neurogenesis (Machon et al., 2007). To address the role of Wnt3a gradients in axonal growth, we used a compartmental microfluidic chamber (MFC) (Taylor et al., 2005). The chamber is composed of a proximal compartment in which the neurons are seeded and a distal compartment. The two compartments are connected by a set of microchannels, allowing the formation of a gradient-based cue of signaling molecules (Figure 3A). We seeded Div0 neurons in MFCs containing either a control-conditioned medium (Ctr-CM) or Wnt3a-conditioned medium (Wnt3a-CM) in the distal compartment. First, we tested whether a proliferative effect of canonical Wnt signaling might bias the comparison of axonal growth in the MFCs. We compared the number of cells between the MFCs containing Ctr-CM and Wnt3a-CM. We found that Wnt3a-CM in the distal compartment did not affect cell proliferation, as the number of cells (defined by nuclei/area) was not different between the two conditions at Div3 (Figure 3B). Furthermore, we observed the clustering of the Wnt co-receptor Lrp6 at the tip of the growing axons (75% of neurons analyzed; n = 12), suggesting a local activation of the canonical Wnt pathway at the axonal tip (Figure 3C). Other components of the Wnt pathway, e.g., β-catenin and Gsk3β, are also enriched at the axonal tip (Figure 3D). Next, we examined whether a spatial gradient of canonical Wnt3a ligands influences axonal growth. We compared the axonal length of neurons seeded in control or Wnt3a

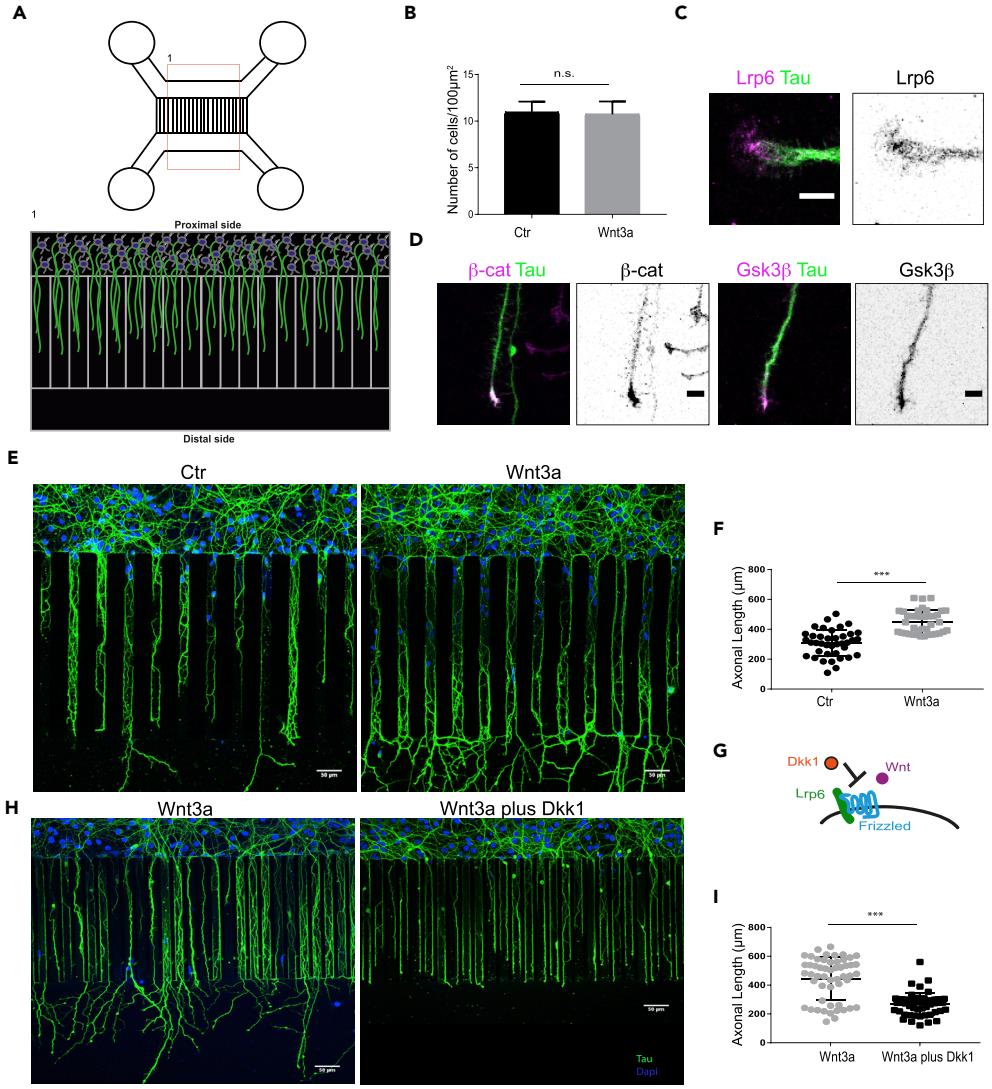

Figure 3. Canonical Wnt Signaling Regulates Axonal Outgrowth

(A) Schematic representation of a two-compartment microfluidic chamber (MFC) used in the study (upper scheme). The lower scheme represents the imaged area (1) with the two compartments, in one compartment (proximal) neurons are seeded in the other compartment (distal) either control-conditioned medium or Wnt3a-conditioned medium is added.

(B) Graph representing the number of neurons per 100 μm^2. Neurons were stained with DAPI, and the number of cells was determined by counting the nuclei. The graph shows the average cell number of three independent experiments ($n > 50$, n.s., not significant, mean (S.E.M.) values are shown).

(C) Neurons were fixed at Div3 and subjected to immunofluorescence staining using antibodies for LRP6 (magenta) and Tau (green). Picture shows LRP6 accumulation at the tip of the axonal growth cone. Left: merged picture of the LRP6 staining and Tau staining. Right: Inverted gray scale of the LRP6 staining. Pictures show representative results of three independent experiments (scale bar, 10 µm).

(D) Neurons in the MFC were fixed at Div3 and subjected to immunofluorescence staining using antibodies for Tau and either β-Catenin or Gsk3β. Left: merged picture of the β-Catenin (magenta) and Tau (green) staining. Middle left: Inverted gray scale of the β-Catenin staining. Middle right: merged picture of the Gsk3β (magenta) and Tau (green) staining. Right: inverted gray scale of the Gsk3β staining (scale bar, 10 µm).

(E) Div0 neurons were seeded in the proximal compartment of the microfluidic chamber; the distal compartment was filled with either control-conditioned medium (left) or Wnt3a-conditioned medium (right). Axons were allowed to grow for 3 days. Afterward, neurons were fixed, stained with antibodies against Tau, and nuclei were counterstained with DAPI. Pictures show representative results of at least three independent experiments (scale bar, 50 µm).

(F) The graph shows the average axonal length of the neurons described in (E) ($n > 30$, ***$p < 0.005$, mean (S.E.M.) values are shown).

Figure 3. *Continued*

(G) Schematic representation of the Dkk1-mediated inhibition of Wnt binding to its co-receptor Lrp6.

(H) Div0 neurons were seeded in the proximal compartment of the microfluidic chamber, the distal compartment was filled with either Wnt3a-conditioned medium (left) or Wnt3a-conditioned medium supplemented with Dkk1 (right). Axons were allowed to grow for 3 days. Afterward, neurons were fixed and stained with antibodies against Tau and nuclei were counterstained with DAPI. Pictures show representative results of at least three independent experiments (scale bar, 50 μm).

(I) The graph shows the average axonal length of the neurons described in (H) ($n > 30$, ***$p < 0.005$, mean (S.E.M.) values are shown).

containing MFCs and revealed a significant increase in the axonal length in neurons exposed to the Wnt3a gradient (Figures 3E and 3F). When neurons where exposed to a reverse gradient, by adding Wnt3a-CM in the proximal side, axons were no longer growing in the distal compartment (Figure S4A), indicating a role of Wnt3a as a directional guidance cue. To verify whether the increased axonal growth is dependent on the activation of canonical Wnt signaling and more specifically on Lrp6, we applied Dkk1 (Figure 3G). Notably, addition of Dkk1 to the Wnt3a-CM in the distal compartment of the MFC strongly reduced axonal growth compared with neurons treated with Wnt3a alone (Figures 3H and 3I). Importantly, the addition of Dkk1 in the proximal compartment does not affect Wnt3a-induced growth (Figure S4B), suggesting once again the directional effect on axonal guidance by canonical Wnts. Considering that Wnt3a guides axon growth between its application on Div0 and measurement at Div3 (Figures 3E and 3F) we further examined whether the same occurs during earlier developmental stages, and indeed we could observe its effect in Div0 to Div2 and Div0 to Div1 (Figure S4C). Therefore, in addition to its involvement in axon establishment and positioning, Wnt3a is a spatial cue that attracts and promotes axonal growth. Gradients of Wnts have been shown to guide commissural axon growth in the spinal cord (Avilés and Stoeckli, 2016). These experiments revealed the function of Wnt3a as a directional and instructive cue for axonal outgrowth. How might Wnt act as a guidance cue? The role of canonical Wnt proteins as guidance cue likely involves its downstream effectors, e.g., APC and Gsk3β, that can directly control microtubule stability (Salinas, 2007), the first step in axonal establishment and growth (Hoogenraad and Bradke, 2009; Witte et al., 2008; Zhou et al., 2004). Alternatively, the local availability of β-catenin could bias the axon to growth in a directional fashion as it is important for the local cross talk of microtubules and actin (Ligon et al., 2001). In addition, β-catenin is a direct interacting partner of N-cadherin, which plays an important role in the first asymmetric events in neurons (Gärtner et al., 2012, 2015). However, further investigation would be necessary to reveal the role of β-catenin in this context. The guidance effect of Wnt3a is mediated by the co-receptor Lrp6 (Figure 3). Recently, it has been shown for commissural axons that Lrp6 has a role in axonal guidance (Avilés and Stoeckli, 2016). Here, we could show that Lrp6 is necessary for axonal growth in hippocampal neurons and likely functions as a co-receptor of Wnt ligands.

Wnt Controls Microtubules Remodeling

Wnt can modulate axonal changes via microtubule re-organization (Salinas, 2007). We observed that Wnt3a has the ability to induce multiple axons, which is also a characteristic phenotype observed by treatment with Taxol (Figure 1A). Hence, we tested whether Wnt3a can directly affect microtubule dynamics during axon specification. To address microtubule dynamics, neurons were transfected with a GFP-MT + Tip construct (GFP-MACF43) and imaged with a spinning disk microscope (Figure 4A). Time-laps movies show that neurons treated with recombinant Wnt3a have a higher number of anterograde comets compared with the control (Figure 4B, red arrows retrograde comets, blue arrows anterograde comets). To confirm these results, kymographs from three different independent experiments were analyzed and the number of anterograde and retrograde comets per neurite per cell was determined (Figure 4C). Although the total number of comets per cell does not change (data not shown), the number of anterograde comets is increased in Wnt3a-treated neurons compared with the control (Figure 4D). These results suggest that Wnt induces plus-end out oriented (anterograde) microtubules, a critical event in axon formation (Yau et al., 2016). Furthermore, kymograph analyses of the axon (Figure 4E) show that comets of Wnt3a-treated neurons are increased in duration (Figure 4F) and run length (Figure 4G), whereas the velocity is unchanged (Figure 4H). These results suggest that Wnt3a signaling shifts the axon microtubule growth dynamics by stabilizing anterograde polymerization in the emerging axon. Consistently, Wnt3a has been shown to affect microtubule directionality at the axonal growth cone (Purro et al., 2008). Inhibition of endogenous Wnt secretion by Iwp-2 did not alter overall anterograde/retrograde microtubule growth balance in Div1 neurites (Figures S5A and S5B), whereas in emerging axons it induced longer time duration but slower growth rate of anterograde comets (Figures S5C–S5E). Although addition of Wnt3a induced a more effective growth (comets lasted longer and grew faster compared with the control), the inhibition of Wnt

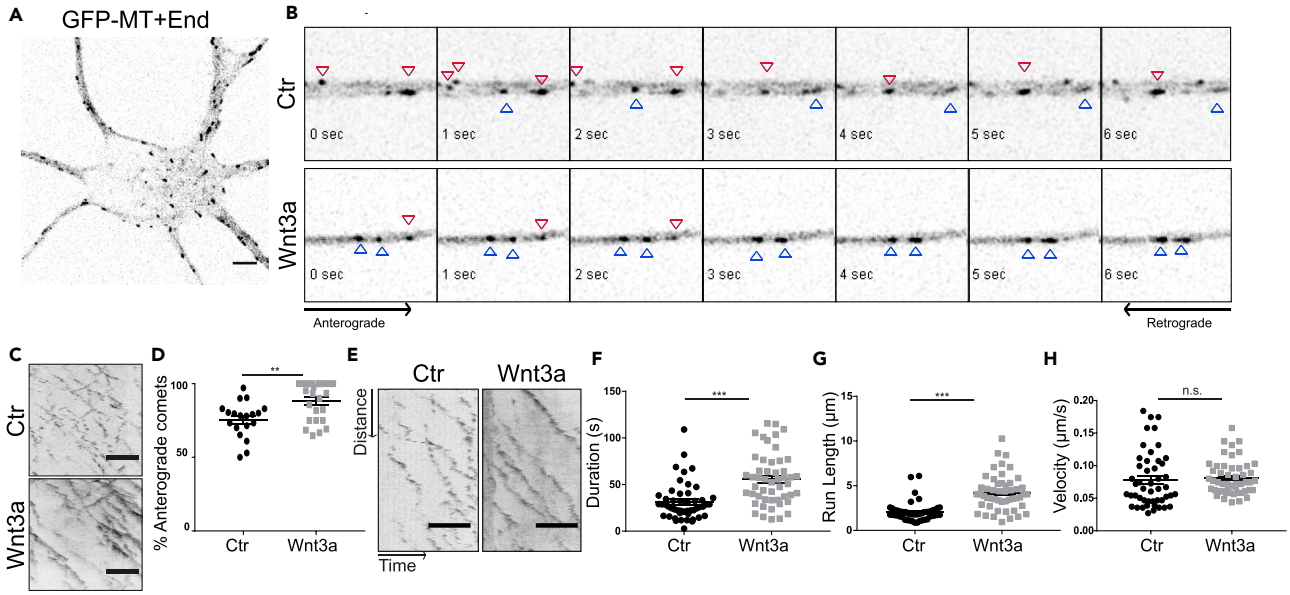

Figure 4. Wnt Influences Axonal Outgrowth by Changing Microtubule Dynamics

Neurons were transfected at Div0 with GFP-MACF43 (GFP-MT + End) and imaged at the spinning disk microscope at Div1 at 1 frame per second.

(A) GFP-MT + End overexpressing neuron at Div1.

(B) Time lapse of retrograde (blue arrowheads) and anterograde (red arrowheads) comets in neurites of untreated neurons (upper panel) or neurons treated with Wnt3a (lower panel).

(C) Representative kymograph of anterograde and retrograde comets of a neurite.

(D) Quantification of the number of retrograde comets in all neurites (n = 20, **p < 0.01, mean (S.E.M.) values are shown).

(E) Representative kymograph of comets in the axon.

(F–H) (F) Quantification of duration, (G) run length, and (H) velocity of the comets (n > 20, ***p < 0.005, mean (S.E.M.) values are shown).

secretion did not lead to a complete opposite effect on microtubule dynamics at this stage; however, it did induce a slower growth rate of microtubules. One possible explanation to this is that the depletion of endogenous Wnt secretion in this early stage of axon development (Div 1) stabilizes the neurites at a premature state of axon development, hence the overall similarity to microtubule dynamics in control condition, whereas excess of Wnt3a accelerates the development of neurites into mature axons by enhancing anterograde microtubule growth.

Based on our results, we propose a model by which the local accumulation of canonical Wnt proteins such as Wnt3a and consequently the local activation of the canonical Wnt pathway controls axonal specification and outgrowth. Although the importance of non-canonical Wnt signaling via the PAR-aPKC complex in these processes is well established (reviewed in (Hapak et al., 2018)), we show that Wnt3a gradients serve as axonal guidance cue through the Wnt co-receptor Lrp6. It would be interesting to address whether other canonical Wnt proteins act in the same manner and furthermore which Frizzled receptors are involved in the observed Wnt3a-mediated effects. Notably, the effects of Wnt3a on axon formation and guidance we observed mimic those of neurotrophin ligands (Nakamuta et al., 2011). Neurotrophin signaling inhibits Gsk3β via PI3K/Akt activation and phosphorylates β-Catenin to promote axon growth in hippocampal neurons (Cross et al., 1995; David et al., 2008; Johnson-Farley et al., 2005). This could suggest a synergistic or additive effect for canonical Wnt and neurotrophin gradient in the guidance of axon development. In summary, the findings we presented reveal an unexplored function of the canonical Wnt pathway in the regulation of neuronal polarity and early stages of axon guidance. This opens up an interesting biological aspect of the canonical Wnt pathway at different levels of neuronal development.

Limitations of the Study

Our findings suggest a fundamental role of canonical Wnt signaling in the establishment of neuronal polarity. However, in this study we were not able to distinguish between cell-autonomous and non-cell-autonomous Wnt signaling. Solving this issue would be important to gain better insight on the role of Wnt as a symmetry breaking signal. A systematic screening of different Wnt molecules and Wnt receptors would be

helpful to understand to which extent specific Wnt ligands or Wnt receptors contribute to neuronal polarity. All experiments were performed *in vitro* on primary neuron cultures. Hence, it would be very important to confirm effects of canonical Wnt signaling on neuronal polarity also *in vivo*, e.g., by using tissue-specific knockout animals or knockin models in which Wnt endogenously tagged.

METHODS

All methods can be found in the accompanying Transparent Methods supplemental file.

SUPPLEMENTAL INFORMATION

Supplemental Information can be found online at https://doi.org/10.1016/j.isci.2019.02.029.

ACKNOWLEDGMENTS

We thank Dr. Gary Davidson for sharing the Lrp6-GFP construct. This work was supported by the Netherlands Organisation for Health Research and Development (ZonMW-TOP, 912.16.058 to CCH, and VICI grant 91815604 and ECHO grant 711.013.012 to MMM), the European Research Council (ERC) (ERC-consolidator, 617050, CCH) and European Molecular Biology Organization (1184-2015 EMBO-ALTF, ES). The work contributed by M.M.M. and I.J. is part of the Oncode Institute, which is partly financed by the Dutch Cancer Society.

AUTHOR CONTRIBUTIONS

E.S. designed the project, performed all experiments, and wrote the manuscript; E.E.Z. and J.S. contributed to the MFC experiments and the revision of the paper; M.B. contributed to the micropattern experiments; M.M.M. and I.J. provided essential reagents, assays, and constructs; L.C.K. supervised the MFC experiments; C.C.H. supervised the project.

DECLARATION OF INTERESTS

The authors declare no competing interests.

Received: March 15, 2018
Revised: September 18, 2018
Accepted: February 26, 2019
Published: March 29, 2019

REFERENCES

van Amerongen, R., and Nusse, R. (2009). Towards an integrated view of Wnt signaling in development. Development *136*, 3205–3214.

Avilés, E.C., and Stoeckli, E.T. (2016). Canonical wnt signaling is required for commissural axon guidance. Dev. Neurobiol. *76*, 190–208.

Bafico, A., Liu, G., Yaniv, A., Gazit, A., and Aaronson, S.A. (2001). Novel mechanism of Wnt signalling inhibition mediated by Dickkopf-1 interaction with LRP6/Arrow. Nat. Cell Biol. *3*, 683.

Bänziger, C., Soldini, D., Schütt, C., Zipperlen, P., Hausmann, G., and Basler, K. (2006). Wntless, a conserved membrane protein dedicated to the secretion of Wnt proteins from signaling cells. Cell *125*, 509–522.

Barnes, A.P., and Polleaux, F. (2009). Establishment of axon-dendrite polarity in developing neurons. Annu. Rev. Neurosci. *32*, 347–381.

Bartscherer, K., Pelte, N., Ingelfinger, D., and Boutros, M. (2006). Secretion of Wnt ligands requires Evi, a conserved transmembrane protein. Cell *125*, 523–533.

Bilic, J., Huang, Y.-L., Davidson, G., Zimmermann, T., Cruciat, C.-M., Bienz, M., and Niehrs, C. (2007). Wnt induces LRP6 signalosomes and promotes dishevelled-dependent LRP6 phosphorylation. Science *316*, 1619–1622.

Cross, D.A.E., Alessi, D.R., Cohen, P., Andjelkovich, M., and Hemmings, B.A. (1995). Inhibition of glycogen synthase kinase-3 by insulin mediated by protein kinase B. Nature *378*, 785–789.

David, M.D., Yeramian, A., Dunach, M., Llovera, M., Canti, C., de Herreros, A.G., Comella, J.X., and Herreros, J. (2008). Signalling by neurotrophins and hepatocyte growth factor regulates axon morphogenesis by differential β-catenin phosphorylation. J. Cell Sci. *121*, 2718–2730.

Dotti, C.G., Sullivan, C.A., and Banker, G.A. (1988). The establishment of polarity by hippocampal neurons in culture. J. Neurosci. *8*, 1454–1468.

Fukumoto, S., Hsieh, C.M., Maemura, K., Layne, M.D., Yet, S.F., Lee, K.H., Matsui, T., Rosenzweig, A., Taylor, W.G., Rubin, J.S., et al. (2001). Akt participation in the Wnt signaling pathway through dishevelled. J. Biol. Chem. *276*, 17479–17483.

Gärtner, A., Fornasiero, E.F., Munck, S., Vennekens, K., Seuntjens, E., Huttner, W.B., Valtorta, F., and Dotti, C.G. (2012). N-cadherin specifies first asymmetry in developing neurons. EMBO J. *31*, 1893–1903.

Gärtner, A., Fornasiero, E.F., and Dotti, C.G. (2015). Cadherins as regulators of neuronal polarity. Cell Adhes. Migr. *9*, 175–182.

Goodman, R.M., Thombre, S., Firtina, Z., Gray, D., Betts, D., Roebuck, J., Spana, E.P., and Selva, E.M. (2006). Sprinter: a novel transmembrane protein required for Wg secretion and signaling. Development *133*, 4901–4911.

Habib, S.J., Chen, B.-C., Tsai, F.-C., Anastassiadis, K., Meyer, T., Betzig, E., and Nusse, R. (2013). A localized Wnt signal orients asymmetric stem cell division in vitro. Science *339*, 1445–1448.

Hapak, S.M., Rothlin, C.V., and Ghosh, S. (2018). PAR3–PAR6–atypical PKC polarity complex

proteins in neuronal polarization. Cell. Mol. Life Sci. *75*, 2735–2761.

Hoogenraad, C.C., and Bradke, F. (2009). Control of neuronal polarity and plasticity–a renaissance for microtubules? Trends Cell Biol. *19*, 669–676.

Inagaki, N., Toriyama, M., and Sakumura, Y. (2011). Systems biology of symmetry breaking during neuronal polarity formation. Dev. Neurobiol. *71*, 584–593.

Johnson-Farley, N.N., Travkina, T., and Cowen, D.S. (2005). Cumulative activation of Akt and consequent inhibition of glycogen synthase kinase-3 by brain-derived neurotrophic factor and insulin-like growth factor-1 in cultured hippocampal neurons. J. Pharmacol. Exp. Ther. *316*, 1062–1069.

Kadowaki, T., Wilder, E., Klingensmith, J., Zachary, K., and Perrimon, N. (1996). The segment polarity gene porcupine encodes a putative multitransmembrane protein involved in Wingless processing. Genes Dev. *10*, 3116–3128.

Kapitein, L.C., and Hoogenraad, C.C. (2015). Building the neuronal microtubule cytoskeleton. Neuron *87*, 492–506.

Lee, S.M., Tole, S., Grove, E., and McMahon, A.P. (2000). A local Wnt-3a signal is required for development of the mammalian hippocampus. Development *127*, 457–467.

Ligon, L.A., Karki, S., Tokito, M., and Holzbaur, E.L.F. (2001). Dynein binds to β-catenin and may tether microtubules at adherens junctions. Nat. Cell Biol. *3*, 913.

Machon, O., Backman, M., Machonova, O., Kozmik, Z., Vacik, T., Andersen, L., and Krauss, S. (2007). A dynamic gradient of Wnt signaling controls initiation of neurogenesis in the mammalian cortex and cellular specification in the hippocampus. Dev. Biol. *311*, 223–237.

Nakamuta, S., Funahashi, Y., Namba, T., Arimura, N., Picciotto, M.R., Tokumitsu, H., Soderling, T.R., Sakakibara, A., Miyata, T., Kamiguchi, H., et al. (2011). Local application of neurotrophins specifies axons through inositol 1,4,5-trisphosphate, calcium, and Ca2+/calmodulin–dependent protein kinases. Sci. Signal. *4*, ra76.

Niehrs, C. (2012). The complex world of WNT receptor signalling. Nat. Rev. Mol. Cell Biol. *13*, 767–779.

Purro, S.A., Ciani, L., Hoyos-Flight, M., Stamatakou, E., Siomou, E., and Salinas, P.C. (2008). Wnt regulates axon behavior through changes in microtubule growth directionality: a new role for Adenomatous Polyposis Coli. J. Neurosci. *28*, 8644–8654.

Salinas, P.C. (2007). Modulation of the microtubule cytoskeleton: a role for a divergent canonical Wnt pathway. Trends Cell Biol. *17*, 333–342.

Stanganello, E., Hagemann, A.I.H., Mattes, B., Sinner, C., Meyen, D., Weber, S., Schug, A., Raz, E., and Scholpp, S. (2015). Filopodia-based Wnt transport during vertebrate tissue patterning. Nat. Commun. *6*, 5846.

Takada, R., Satomi, Y., Kurata, T., Ueno, N., Norioka, S., Kondoh, H., Takao, T., and Takada, S. (2006). Monounsaturated fatty acid modification of Wnt protein: its role in Wnt secretion. Dev. Cell *11*, 791–801.

Taylor, A.M., Blurton-Jones, M., Rhee, S.W., Cribbs, D.H., Cotman, C.W., and Jeon, N.L. (2005). A microfluidic culture platform for CNS axonal injury, regeneration and transport. Nat. Methods *2*, 599–605.

Witte, H., Neukirchen, D., and Bradke, F. (2008). Microtubule stabilization specifies initial neuronal polarization. J. Cell Biol. *180*, 619–632.

Yan, D., and Lin, X. (2009). Shaping morphogen gradients by proteoglycans. Cold Spring Harb. Perspect. Biol. *1*, a002493.

Yau, K.W., Schatzle, P., Tortosa, E., Pages, S., Holtmaat, A., Kapitein, L.C., and Hoogenraad, C.C. (2016). Dendrites in vitro and in vivo contain microtubules of opposite polarity and axon formation correlates with uniform plus-end-out microtubule orientation. J. Neurosci. *36*, 1071–1085.

Zhai, L., Chaturvedi, D., and Cumberledge, S. (2004). Drosophila wnt-1 undergoes a hydrophobic modification and is targeted to lipid rafts, a process that requires porcupine. J. Biol. Chem. *279*, 33220–33227.

Zhou, F.-Q., Zhou, J., Dedhar, S., Wu, Y.-H., and Snider, W.D. (2004). NGF-induced axon growth is mediated by localized inactivation of GSK-3β and functions of the microtubule plus end binding protein APC. Neuron *42*, 897–912.

ISCI, Volume *13*

Supplemental Information

Wnt Signaling Directs Neuronal Polarity and Axonal Growth

Eliana Stanganello, Eitan Erez Zahavi, Mithila Burute, Jasper Smits, Ingrid Jordens, Madelon M. Maurice, Lukas C. Kapitein, and Casper C. Hoogenraad

Figure S1

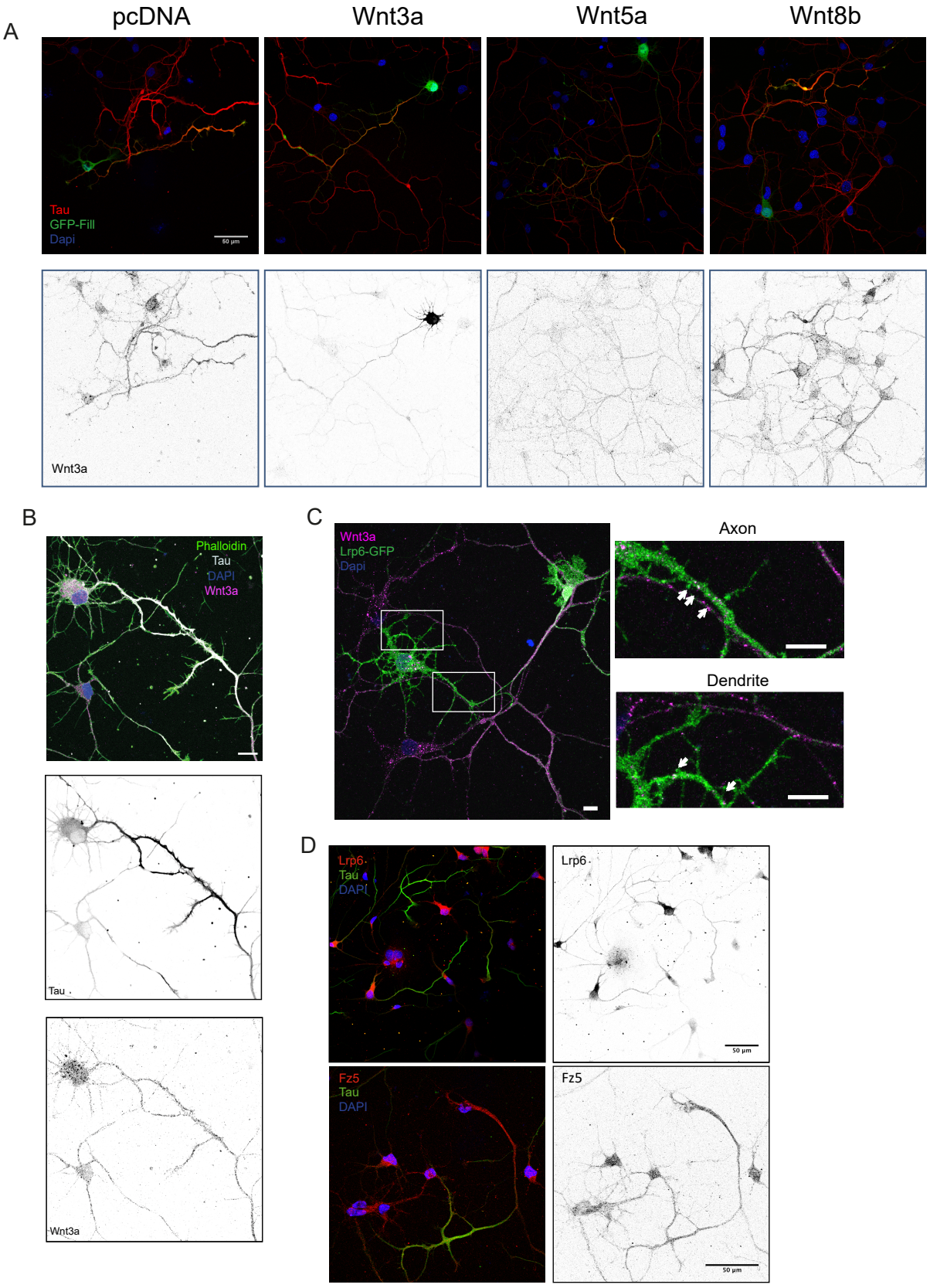
A
pcDNA
Wnt3a
Wnt5a
Wnt8b
Tau
GFP-Fill
Dapi
Wnt3a
B
Phalloidin
Tau
DAPI
Wnt3a
Tau
Wnt3a
C
Wnt3a
Lrp6-GFP
Dapi
Axon
Dendrite
D
Lrp6
Tau
DAPI
Lrp6
Fz5
Tau
DAPI
Fz5

Figure S1. Related to Figure 1. Overview of Wnt3a and LRP6 distribution in hippocampal neurons

A) Neurons were transfected with a GFP expression plasmid mixed with either pCDNA3, Wnt3a, Wnt5a or Wnt8B plasmids on Div0, then fixed and immunostained on Div2 against Tau and Wnt3a. Nuclei were counterstained with DAPI. (scale bar= 50µm).

B) Neurons were fixed at Div2, stained with antibodies against Wnt3a (magenta) and Tau (grey). Neurons were counterstained with Phalloidin (actin filaments; green) and DAPI (nuclei; blue) (left side: merged picture; right side: inverted gray scale channel of the endogenous Wnt3a expression and Tau (scale bar =10µm).

C) Neurons were transfected at Div3 with Lrp6-GFP, fixed at Div4 and stained for Wnt3a (magenta). Neurons were counterstained with DAPI (nuclei; blue). Overview picture of the Lrp6-GFP overexpressing neuron (left) from Figure 1B. The white boxes indicate the zoom-in of the axon and of a dendrite. Signalosome (co-localization between Wnt3a and Lrp6) are indicated with the white arrows.

D) Neurons were fixed at Div4, stained with antibodies against Lrp6 (upper panel) Fz5 (lower panel) and Tau (green). Neurons were counterstained DAPI (nuclei; blue) (left side: merged picture; right side: inverted gray scale channel of the endogenous Lrp6 and Tau.

Figure S2

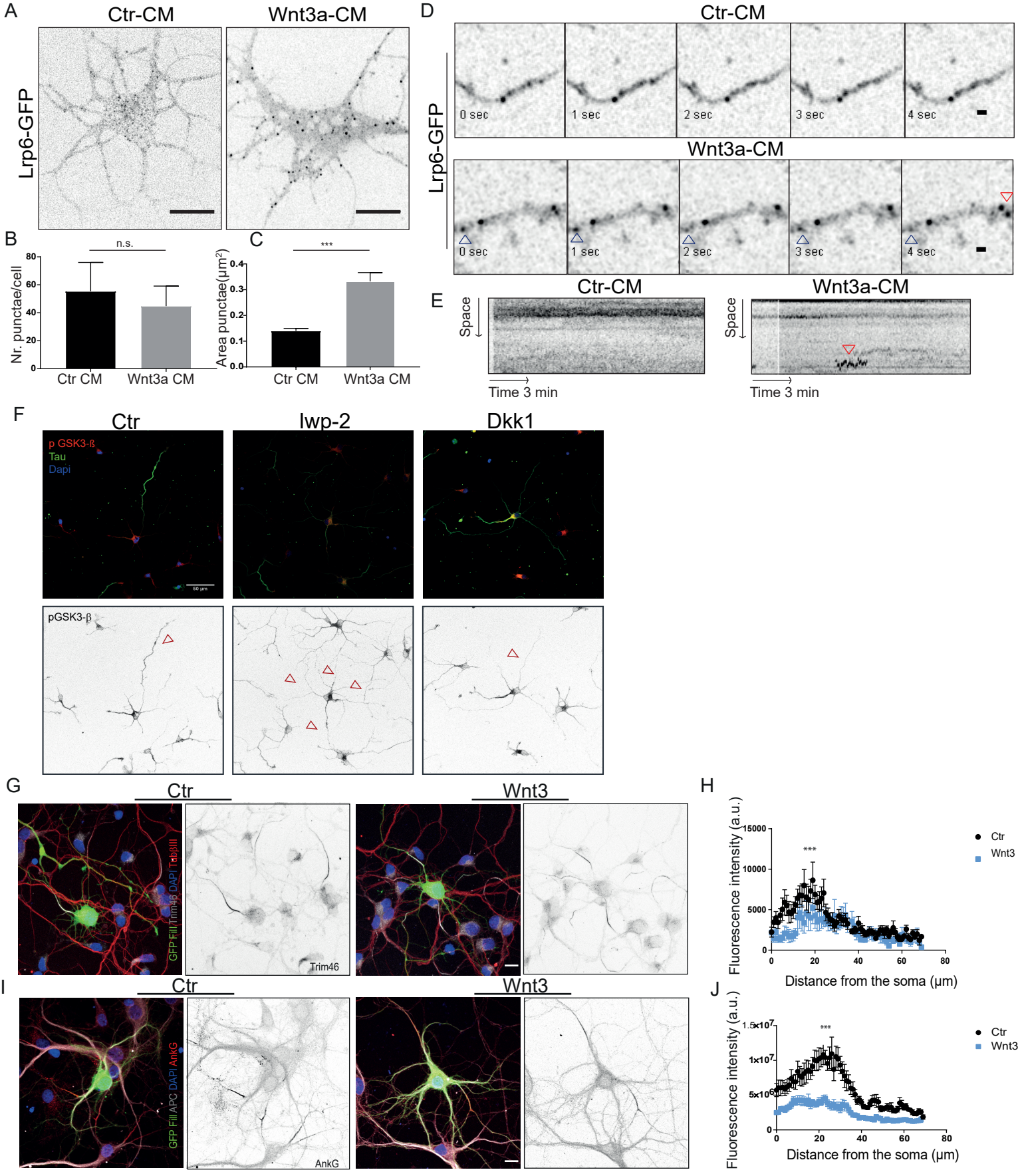
A
Ctr-CM
Wnt3a-CM
Lrp6-GFP
B
n.s.
Nr. punctae/cell
Ctr CM
Wnt3a CM
C
***
Area punctae(µm²)
Ctr CM
Wnt3a CM
D
Ctr-CM
Lrp6-GFP
0 sec
1 sec
2 sec
3 sec
4 sec
Wnt3a-CM
E
Ctr-CM
Wnt3a-CM
Space
Time 3 min
F
Ctr
Iwp-2
Dkk1
p GSK3-β
Tau
Dapi
pGSK3-β
G
Ctr
Wnt3
GFP Fill Trim46 DAPI Tubβ III
Trim46
H
Fluorescence intensity (a.u.)
Distance from the soma (µm)
Ctr
Wnt3
I
Ctr
Wnt3
GFP Fill APC DAPI AnkG
AnkG
J
Fluorescence intensity (a.u.)
Distance from the soma (µm)
Ctr
Wnt3

Figure S2. Related to Figure 1 and Figure 2. Wnt3a accumulation at the axon induces Lrp6 clustering and influences localization of AIS protein

A-E) Neurons were transfected at Div3 with Lrp6-GFP, at Div4 they were treated for 30 min with Wnt3a-CM or Ctr-CM and imaged at the spinning disk microscope.

A) Lrp6 clusters formation in neurons treated with Ctr-CM (left) and Wnt3a-CM (right) (scale bar =10µm).

B) Bar graph quantifying the number of puncta per cell (n=5) (n.s.=not significant).

C) Quantification of the area of the punctae (n=5) (***p<0.005).

D) Time lapse of Lrp6-cluster dynamics (1 frame per second) in the proximal axon of neuron treated with Ctr-CM (upper panel) and Wnt3a-CM (lower panel) (scale bar =2µm).

E) Kymograph of Lrp6 punctae in a Ctr-CM treated neuron (left) and Wnt3a-CM treated neuron (right).

F) Neurons were either left untreated or treated at Div0 with Iwp-2, or recombinant Dkk1 (100ng/ml). At Div2 neurons were fixed and stained for Tau, pGsk3β (inactive state) and counterstained with DAPI. Upper panel: Merged staining of Tau proteins (green), inactive Gsk3β (red) and nuclei (DAPI; blue). Lower panel: Inverted gray scale of intensity of the antibody staining against pGsk3β. Experimental conditions from left to right: untreated neurons, neurons treated with Iwp-2 and recombinant Dkk1. Pictures show representative results of at least 3 independent experiments (scale bar =50 µm). Red arrows heads indicate pGsk3β positive neurites.G-J) Neurons were co-transfected with a GFP-Fill (green) and an empty vector or Wnt3 at Div0.

G) Transfected neurons were fixed at Div4. On the left control neurons stained for Trim46 (gray), TubulinβIII (red) and DAPI (blue)(merged picture left), inverted gray scale of Trim46 staining (right). On the right, Wnt3 transfected neurons stained for Trim46 (gray), Tubulin-βIII (red) and DAPI (blue) (merge picture left), inverted gray scale of Trim46 staining (right) (scale bar =10µm).

H) Quantification of the intensity profile of Trim46 in the axonal initial segment (n=12,***p<0.005).

I) Transfected neurons were fixed at Div8. On the left control neurons stained for AnkG (red), APC (gray) and DAPI (blue)(merge picture left), inverted gray scale of AnkG staining (right). On the right side Wnt3 transfected neurons stained for AnkG (red), APC (gray) and DAPI (blue) (merge picture left), inverted gray scale of AnkG staining (right) (scale bar =10µm).

J) Quantification of the intensity profile of AnkG in the axonal initial segment (n=12, ***p<0.005).

Figure S3

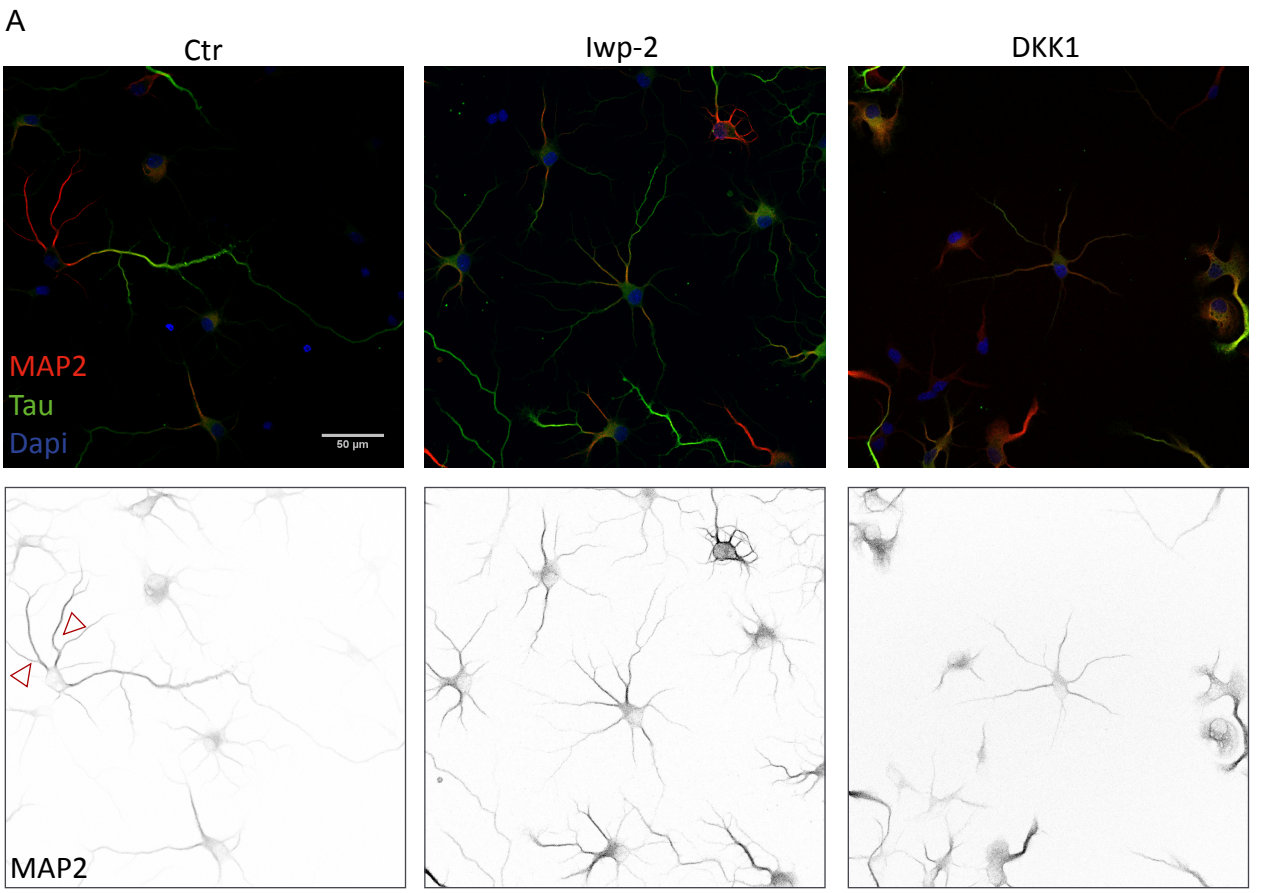
A
Ctr
Iwp-2
DKK1
MAP2
Tau
Dapi
50 µm
MAP2

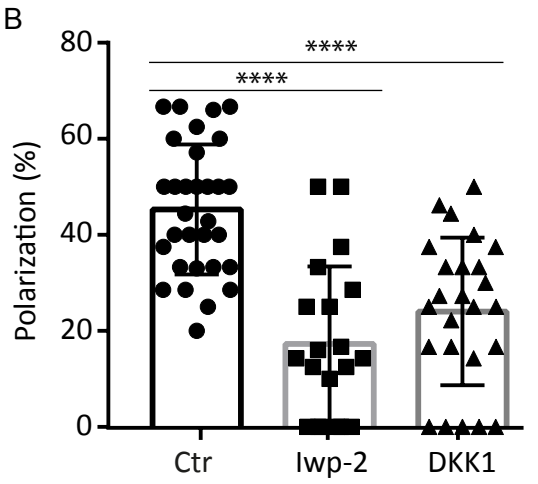
B
Polarization (%)
80
60
40
20
0
****
****
Ctr
Iwp-2
DKK1

Figure S3. Related to Figure 2. Inhibition of Wnt3a signaling induces mislocalization of Tau and MAP2

A) Neurons were either left untreated (left), treated with the inhibitor of Porcupine Iwp-2 (1µM) (middle) or the antagonistic inhibitor of the LRP6-Wnt3a interaction Dkk1 (100ng/ml) (right), respectively. Treatments were added on Div0 and the neurones were fixed on Div2. The neurons were stained for MAP2 (red), Tau (green) DAPI (blue). Below is the inverted gray scale of the intensity of the antibody staining against MAP2. The red arrows show the dendrites, enriched with MAP2 in the untreated condition. Pictures show representative results of at least 3 independent experiments for control and Iwp-2 and 2 for Dkk1 (scale bar = 50 µm).

B) graph representing the percentage of polarized neurons in each condition. Neurons with a correct localization of Tau in one of the neurites were counted as polarized. The pictures taken of each condition were quantified and normalized to the amount of healthy nuclei present in the picture and were taken randomly throughout the coverslip (****$p<0.001$). The graph shows the mean with standard deviation.

Figure S4

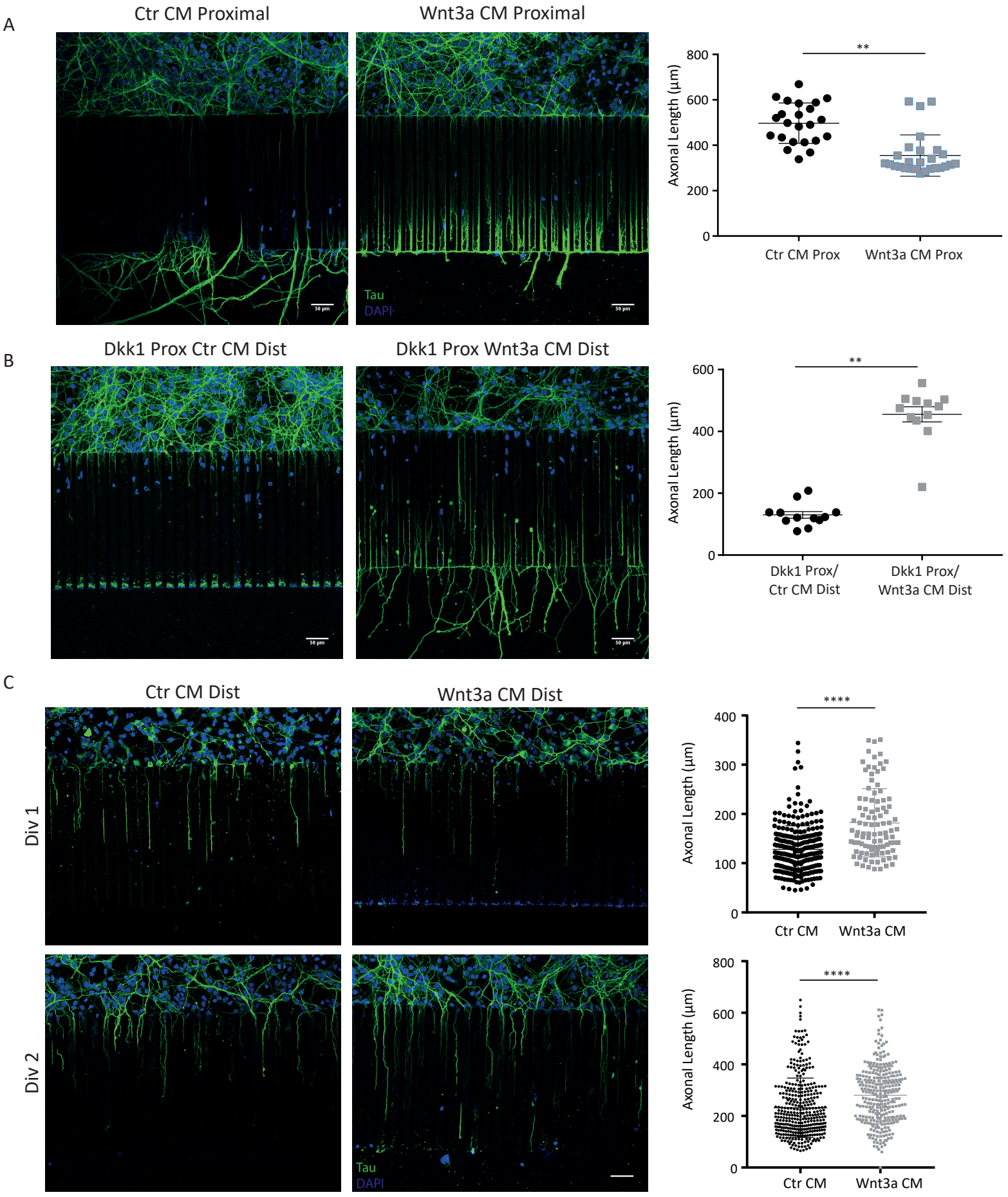
A
Ctr CM Proximal
Wnt3a CM Proximal
Tau
DAPI
Axonal Length (µm)
800
600
400
200
0
**
Ctr CM Prox
Wnt3a CM Prox
B
Dkk1 Prox Ctr CM Dist
Dkk1 Prox Wnt3a CM Dist
Axonal Length (µm)
600
400
200
0
**
Dkk1 Prox/
Ctr CM Dist
Dkk1 Prox/
Wnt3a CM Dist
C
Ctr CM Dist
Wnt3a CM Dist
Div 1
Div 2
Tau
DAPI
Axonal Length (µm)
400
300
200
100
0
****
Ctr CM
Wnt3a CM
Axonal Length (µm)
800
600
400
200
0
****
Ctr CM
Wnt3a CM

Figure S4. Related to Figure 3. Wnt3a acts as an early guidance cue

A) Div0 neurons were seeded in the proximal compartment of the microfluidic chamber and it was filled with either control-conditioned medium (left) or Wnt3a-conditioned medium (right). Axons were allowed to grow for 3 days. Afterwards, neurons were fixed, stained with antibodies against Tau and nuclei were counterstained with DAPI. Pictures show representative results of at least 3 independent experiments (scale bar =50 µm). Graph shows the average axonal length of the neurons (**$p<0.01$).

B) Neurons were seeded as in (A) and recombinant Dkk1 100 ng/ml was added, the distal compartment was filled with either control conditioned medium (left) or Wnt3a-conditioned medium (right). Axons were allowed to grow for 3 days. Afterwards, neurons were fixed and stained as in (A). Pictures show representative results of at least 3 independent experiments (scale bar =50 µm). Graph shows the average axonal length of the neurons) (**$p<0.01$).

C) Neurons were seeded as in (A) and the distal compartment was filled with Wnt3a or control-conditioned media. Neurons were fixed after 1 or 2 days (Div1 & Div2) then stained as in (A). Pictures show representative results of at least 3 independent experiments (scale bar =50 µm). Graph shows the average axonal length of the neurons) (n= number of axons measured. Div1 Ctr n=278, Div1 Wnt3a n=100, Div2 Ctr n=365, Div2 Wnt3a n=291. ****$p<0.0001$).

Figure S5

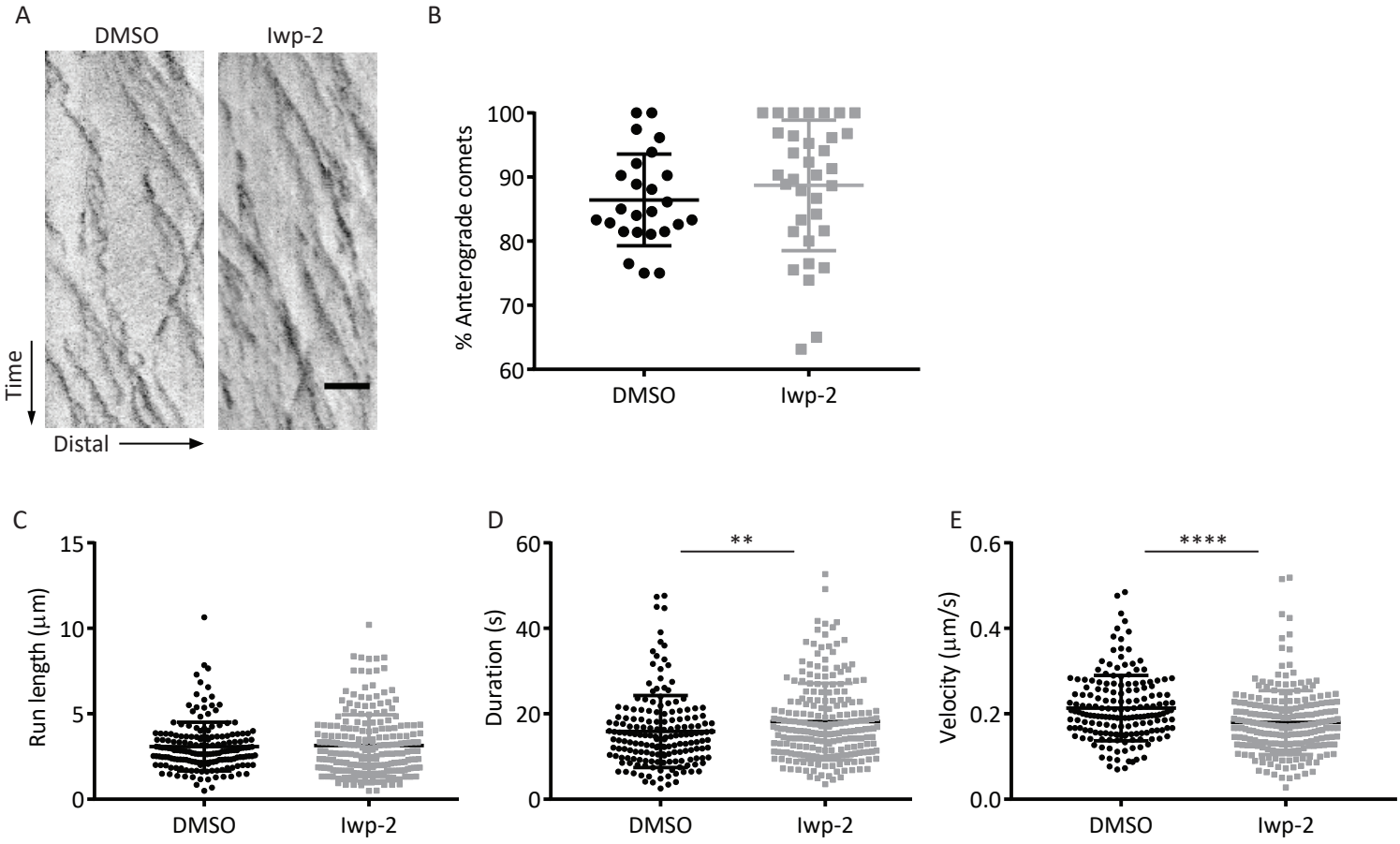
A
DMSO
Iwp-2
Time
Distal
B
% Anterograde comets
100
90
80
70
60
DMSO
Iwp-2
C
Run length (µm)
15
10
5
0
DMSO
Iwp-2
D
Duration (s)
60
40
20
0
**
DMSO
Iwp-2
E
Velocity (µm/s)
0.6
0.4
0.2
0.0
****
DMSO
Iwp-2

Figure S5. Related to Figure 4. Inhibition of Wnt secretion affects microtubule dynamics

A-E) Neurons were transfected at Div0 with mCherry-MACF43 (GFP-MT+ End) and imaged at the spinning disk microscope at Div1. Immediately after transfection, neurons were treated with Iwp-2 or DMSO 0.1% as control. Results are based on two independent experiments.

A) Representative kymographs of neurites in Iwp-2 and DMSO treated neurons. Time duration is 2 minutes. Scale bar= 5µm.

B) Average percentage of anterograde comets per all neurites measured (n= 25 & 34 for DMSO & Iwp-2 respectively).

C-E) A single neurite per neuron with the highest anterograde comet percentage was selected as the designated future axon. Run length, duration and velocity were calculated per comet (n= 174 & 224 comets for DMSO & Iwp-2, **$p<0.01$, ****$p<0.001$).

Transparent Methods

Ethic Statement

All experiments with animals were performed in compliance with the guidelines for the welfare of experimental animals issued by the Government of the Netherlands, and were approved by the Animal Ethical Review Committee (DEC) of Utrecht University.

Hippocampal neuron cultures, transfections and drug treatments

Primary hippocampal and cortical cultures were prepared from embryonic day 18 rat brains (both genders). Cells were plated on coverslips coated with poly-L-lysine (PLL, 37,5 mg/mL) and laminin (1,25 mg/mL) at a density of 100.000/well. Neurons were cultured in complete Neurobasal medium (NB) supplemented with 2% B27 (GIBCO), 0,5 mM glutamine (GIBCO), 15,6 mM glutamate (Sigma), and 1% penicillin/streptomycin (GIBCO) at 37 °C. For transfection 1,8 µg DNA/coverslip was incubated with 3,3 µl of Lipofectamine 2000 (Thermofisher, 11668019) in 200µl of NB for 30 min and added to the neuron in NB supplemented with 0,5 mM glutamine for 45 min. After this step, neurons were briefly washed and transferred back to the original medium. The following constructs have been used: β-tubulin-GFP (kind gift from Dr. P. Schätzle), GFP-Macf43 (Yau et al., 2014), Lrp6-GFP (kind gift from Dr. Gary Davidson), Wnt3a-FT (Farin et al., 2016), Wnt3 (Addgene, #35909).

Treatment of neurons with drugs and recombinant proteins

To induce multiple axons formation, neurons were treated with 10nM Taxol (Sigma-Aldrich, T7402) for 48h. The treatment was started at day *in vitro* (Div) 2 and neurons were fixed with 4% paraformaldehyde (PFA) at Div 4. To block Wnt secretion, neurons were treated on Div0 with 1 µM Iwp-2 (STEMCELL technologies, 72122,) and fixed with 4% PFA at indicated time points (see figure legends). To induce Wnt-signaling, neurons were stimulated with 40 ng/ml Wnt3a (R&D System, 1324-WN, time points are indicated in figure legends). Dkk1 (R&D System 5897-DK) was used at a concentration of 100 ng/ml.

Micropattern

Glass coverslips (VWR #631) were plasma activated (Harrick Plasma Cleaner) for 1 min at high intensity settings and then coated with Poly (L-Lysine)-graft-Poly (Ethylene Glycol) (PLL-PEG) (SuSoS, Switzerland) solution of 0.1 mg/ml in HEPES 10mM pH 7.4 for 30 minutes at room temperature (R.T.). Coverslips were washed in milliQ water, placed onto a photomask and then insolated under a deep UV lamp (Jelight, #42-220) for 4 min. The micropttern geometries were 10µm wide and 300µm in length (lines, Fig. 2F). Coverslips were

incubated for 2 hours at R.T. with 40µM BSA conjugated with Alexa Fluor 647 (ThermoFisher, #A34785) alone or in combination with 100 ng/ml of recombinant Wnt3a (R&D System, 1324-WN). After this step, coverslips were washed and coated with poly-L-Lysine (37.5 mg/ml). Neurons were plated at a density of 50.000 cells per coverslip. Neurons were manually categorized as described in Fig. 2E.

Microfluidic chamber (MFC)

MFC made of Sylgard 184© polydimethylsiloxane (PDMS) were cast and prepared as described previously, with minor alteration, based on the small-form factor design mold of two-compartment chamber (Taylor et al., 2005). Briefly, PDMS was mixed with curing agent at 10:1 w/w ratio and cast on Epoxy-resin molds. Cured PDMS devices were cut and four 5-mm wells were punched in the ends of the channels of both compartments. Devices were adhered to coverslips by plasma-cleaner activation (Harrick Plasma), then treated with pLL plus Laminin mixture to enable neuron attachment. Hippocampal neurons were plated at a density of 150.000/MFC in an initial volume of 4µl in one well of the MFC (proximal site). After 30 minutes of incubation 50 µl/microwell complete NB medium (supplemented as indicated for the neuron cultures) was added in the proximal compartment (on the same side where neurons were seeded). On the opposite side (distal compartment) complete NB medium was diluted 1:1 with either control- conditioned medium (Ctr-CM), Wnt3a-conditioned medium (Wnt3a-CM) or Wnt3a- conditioned media plus 100 ng/ml Dkk1 and added to the distal microwells (60 µl/microwell).

Wnt3a-conditioned media

L-cells (ATCC CRL-2648) were cultured in DMEM containing 1 g/l glucose (Life Technologies), supplemented with 10% FCS and P/S. All cells were maintained at 37 °C in 5% CO2. L-cells stably expressing and secreting Wnt3a or Wnt3a-FlagTag were cultured in the presence of 125 µg/ml Zeocine (Life Technologies) to obtain Wnt3a-conditioned medium (Shibamoto et al., 1998).

Immunofluorescence staining and imaging

Fixed cells were washed 3 times for 5 min in PBS, permeabilized in 0.25% TritonX-100, incubated for an hour at R.T. with BSA 2% and after with the primary-antibody in GDB buffer (0.2% BSA, 0.8 M NaCl, 0.5% Triton X-100, 30 mM phosphate buffer, pH 7.4) overnight at 4°C. After 3 times washing with PBS, cells were incubated with secondary-antibodies in GDB buffer for an hour at R.T. After washing, coverslips were mounted in Vectashield), Vectashield antifade mounting medium with DAPI (Vectorlabs, H-1200). The primary antibodies used were: rabbit anti-TRIM46 [37] rabbit anti-β-III tubulin (Covance, AB_291637), mouse anti-β-III tubulin (Sigma AB_082M4845), mouse anti- dephosphorylated Tau (clone PC1C6,

Chemicon, AB_94855), rabbit anti-MAP2 (Cell Signaling, CST_4542), mouse anti-AnkirinG (Zymed, Life technologies AB_33-8800), rabbit anti-Wnt3 (Abcam AB_28472), rabbit anti β-catenin (Abcam AB_32572), rabbit anti-Frizzled5 (Abcam AB_75234), rabbit anti-LRP6 (Abcam AB_66156), rabbit anti-phospho Ser9 Gsk3 β (Cell Signaling, AB_9323). Secondary antibodies: anti-mouse Alexa488 (Life Technologies, AB_2534088), anti-rabbit Alexa488 (Life Technologies, A11034, RRID: AB_2576217), anti-mouse Alexa568 (Life Technologies A11031, RRID: AB_144696), anti- rabbit Alexa568 (Life Technologies, A11036, RRID: AB_10563566), anti-mouse Alexa647 (Life Technologies A21236, RRID: AB_2535805), anti-rabbit Alexa647 (Life Technologies, A21245, RRID: AB_2535813). Neurons were imaged with a LSM700 confocal laser-scanning microscope (Zeiss) with a Plan-Apochromat 63x NA 1.40 oil DIC, EC Plan-Neofluar 40x NA1.30 Oil DIC and a Plan-Apochromat 20x NA 0.8 objective. Each confocal image was a z series of 5–10 images, each averaged 4 times, covering the entire region of interested from top to bottom. Maximum projections were done from the resulting z stack. For fluorescence intensity comparison, settings were kept the same for all conditions.

Live-cell imaging

Live-cell imaging experiments were performed in an inverted microscope Nikon Eclipse Ti-E (Nikon), equipped with a Plan Apo VC 100x NA 1.40 oil and a Plan Apo VC 60x NA 1.40 oil objective (Nikon), a Yokogawa CSU-X1-A1 spinning disk confocal unit (Roper Scientific), a Photometrics Evolve 512 EMCCD camera (Roper Scientific) and an incubation chamber (Tokai Hit) mounted on a motorized XYZ stage (Applied Scientific Instrumentation) which were all controlled using MetaMorph (Molecular e5 Neuron 94, 809–825.e1–e7, May 17, 2017). Quantification of moving particles length (length of the comet run (C) multiplied by sin (α) where α is 90 minus the angle created by the comet truck and a horizontal line), duration (C* cos(α)) , and velocity (tan (α)) of dynamic microtubules (labeled with GFP-MACF43), were quantified from kymographs of proximal axons created using the Kymoreslicewide plug- in under Fiji (https://github.com/ekatrukha/KymoResliceWide) under ImageJ (NIH, https://imagej.nih.gov/ij/). Lrp6 punctae counting and area measurements were performed using the Analyze Particle function of Image J. Axonal length was calculated by drawing in ImageJ a segmented line along the axon starting from the beginning of the channel to the end of the field of view.

Quantification and Statistical Analysis

All statistical details of experiments, including the definitions and exact values of n, and statistical tests performed, can be found in Figures and Figure Legends. Data processing and statistical analysis were done in Excel and GraphPad Prism (GraphPad Software). Significance

was defined as: ns-not significant, $^{*}p < 0.05$ $^{**}p < 0.01$ and $^{***}p < 0.001$. Statistical analysis: Unpaired t test.

Supplemental References

Farin, H.F., Jordens, I., Mosa, M.H., Basak, O., Korving, J., Tauriello, D.V.F., de Punder, K., Angers, S., Peters, P.J., Maurice, M.M., et al. (2016). Visualization of a short-range Wnt gradient in the intestinal stem-cell niche. Nature *530*, 340.

Shibamoto, S., Higano, K., Takada, R., Ito, F., Takeichi, M., and Takada, S. (1998). Cytoskeletal reorganization by soluble Wnt-3a protein signalling. Genes to Cells *3*, 659–670.

Taylor, A.M., Blurton-Jones, M., Rhee, S.W., Cribbs, D.H., Cotman, C.W., and Jeon, N.L. (2005). A microfluidic culture platform for CNS axonal injury, regeneration and transport. Nat. Methods *2*, 599–605.

Yau, K.W., van Beuningen, S.F.B., Cunha-Ferreira, I., Cloin, B.M.C., van Battum, E.Y., Will, L., Schätzle, P., Tas, R.P., van Krugten, J., Katrukha, E.A., et al. (2014). Microtubule minus-end binding protein CAMSAP2 controls axon specification and dendrite development. Neuron *82*, 1058–1073.